Test campaign and performance evaluation of a spiral latent storage module with Hitec® as PCM

M.M. Rodriguez-Garcia[1], E. Rojas[2] and R. Bayón[2]

[1] Ciemat - Plataforma Solar de Almería, Almería (Spain)

[2] Ciemat - Plataforma Solar de Almería, Madrid (Spain)

Abstract

A modified spiral plate heat exchanger for its use as thermal energy storage (TES) has been selected using Hitec® salt as storage medium within the activities of the REELCOOP project (7th Framework program of the European Union Ref N. 608466, www.reelcoop.com). After its installation at one of the storage test facility at PSA (Plataforma Solar of Almería) and its commissioning, the test campaign has been performed. The testing procedures and the results evaluation are presented in this paper. For a better understanding of the phase change process, thermal analyses of the commercial Hitec® salt have been carried out.

Keywords: Latent storage, spiral heat exchanger, Hitec® as phase change material.

1. Introduction

A modified design based on a spiral plate heat exchanger used as latent thermal energy storage module was proposed in the Prototype #3 of the REELCOOP project. In this project an organic ranking cycle (ORC) using parabolic trough solar collectors is to be driven with direct steam generation combined with a biogas boiler. In order to keep producing power in the necessary transient time to change from solar field to biomass boiler a latent storage module was included as part of this plant. The reliable phase change material (PCM) used to meet the temperature range needed for both ORC and solar field is the Hitec® salt.

Previous results regarding the phase change material selection were presented by Rodriguez-Garcia et al., 2016a, where several candidates PCMs in the range of 130 ºC to 170 ºC were studied. The commercial Hitec® salt was selected because it was the only one that showed chemical stability under cycling and despite its relatively low phase change enthalpy.

In the EuroSun congress (Rodriguez-Garcia and Rojas, 2016b) the settlement of the problems addressed during the commissioning was presented: mainly the filling of the spiral thermal energy storage module and the presence of water remaining from a previous mandatory pressure test.

In this paper the test campaign of the spiral storage module with Hitec® salt as PCM and a preliminary evaluation of the results are presented. Moreover, further thermal analyses of Hitec® like differential scanning calorimetry (DSC) measurements, melting/freezing cycles in the oven under air down to 40 ºC together with the analysis of salt composition after the cycles are presented as well.

2. Facility description

Patented by Rivas et al. (2011), the module tested in the REELCOOP project is an adaptation of a commercial spiral plate heat exchanger, due to limitations in budget and project time frame. With 825 mm external diameter and 1000 mm height, the spiral heat exchanger used as TES module has volume at the water/steam channel of 205 liters, and 230 liters at the molten salt channel. For more information see Rodriguez-Garcia and Rojas, 2016b.

The testing facility was designed to operate in both charging (see Fig. 1(a)) and discharging modes (see Fig. 1(b)) with water as heat transfer fluid (HTF). In nominal conditions, for the charging (discharging) mode a steam generator (water heater) provides saturated steam (warm water) to the storage module where energy is transferred to (from) the PCM. The storage module provides a mixture of steam and liquid water in an undetermined ratio or steam quality. This water-steam flow is later mixed with liquid water at known temperature and flow. The resulted

doi:10.18086/swc.2017.14.06 Available at http://proceedings.ises.org

water-liquid flow and its temperature are measured and the thermal cycle is closed.

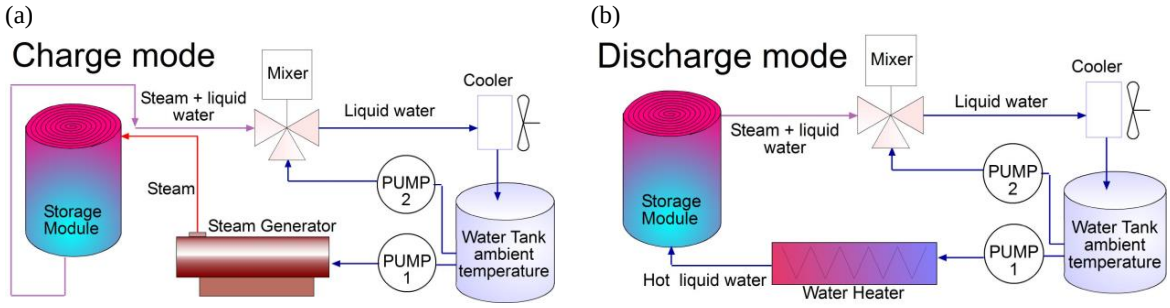

Fig. 1 Charge (a) and discharge (b) operation mode schemas of the test facility at Plataforma Solar de Almería. The facility is composed by: a water tank; a steam generator that provides saturated steam; an electric water heater; two pumps; a mixer; and a water cooler.

The pressure in the whole loop is given by the steam generator in charge or by the boiler in discharge and controlled by a pressure regulating valve situated at the mixed inlet. A 0.5 MPa pressure drop was calculated.

Theoretically, during the charge operation saturated steam at 150 °C enters the storage module prototype (TES) through the A2 conduction (see Fig. 2) and, once the heat is transferred to the PCM, saturated water at 140 °C exits the TES module through the A1 pipeline. During the discharge, the operation takes place in the contrary flow direction: saturated water at 130 °C enters the TES through the A1 conduction and, after evaporating in the TES, saturated steam at 130 °C leaves the module through A2. Tab. 1 shows a summary of the nominal operation conditions for both charge and discharge modes.

Tab. 1: Nominal operation conditions for the charge and discharge modes at TES module.

Charge mode				
	Temperature [°C]	Pressure [MPa]	Flow [kg/s]	Water phase
Inlet (A2)	150	0.47	0.04	Saturated steam
Outlet (A1)	140	0.36	0.04	Saturated water
Discharge mode				
	Temperature [°C]	Pressure [MPa]	Flow [kg/s]	Water phase
Inlet (A1)	130	0.27	0.05	Saturated water
Outlet (A2)	130	0.26	0.05	Saturated steam

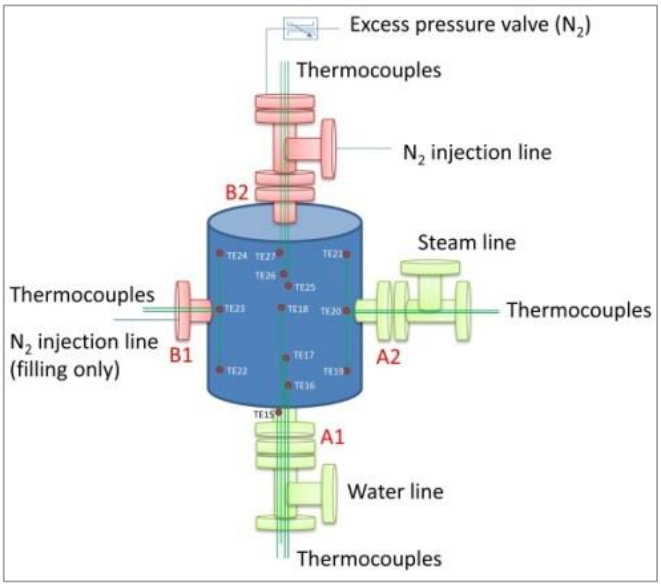

Fig. 2: TES module temperature sensors.

While water flow is measured with vortex flowmeters, steam flow is measured with a Coriolis-type flowmeter. The storage module tested here did not allow including temperature gauges at different radial positions, but at the center and outer radius of the equipment. The final distribution is shown in Fig. 2.

3. Storage module test campaign

After commissioning, test campaign took place from 23/11/2016 to 15/01/2017. The most remarkable aspects of the preoperational tests and the TES module filling with the selected PCM where presented in Rodriguez-Garcia and Rojas, 2016b. In this section, the thermal performance tests are presented, comparing the results with that theoretically expected. While January, 9th has been taken as reference day, the most important results are also observed in the rest of the days. A further work will present the details of repeatability and quality of the whole test campaign.

3.1. Charge mode

In this operation mode water should go into the storage module as saturated steam through the lateral upper entrance (A2 in Fig. 2) and flow through the spiral channel from the largest diameter to the smallest one. Along its way, water is expected to loss energy by melting the solid PCM, placed in the alternate spiral channel, and to condensate. The saturated water should be drained by gravity to the bottom.

During the commissioning testing days, some experience had to be acquired to control pressure and temperature inside the TES module. PCM temperature gauges showed the PCM did not melt when operating at nominal conditions, and hence, a change in the operation strategy had to be adopted by having 170 °C set point for the steam generator and adjusting the circuit pressure to the corresponding saturated steam pressure (0.89 MPa). Nominal mass flow was not achieved due to limitations in the steam generator.

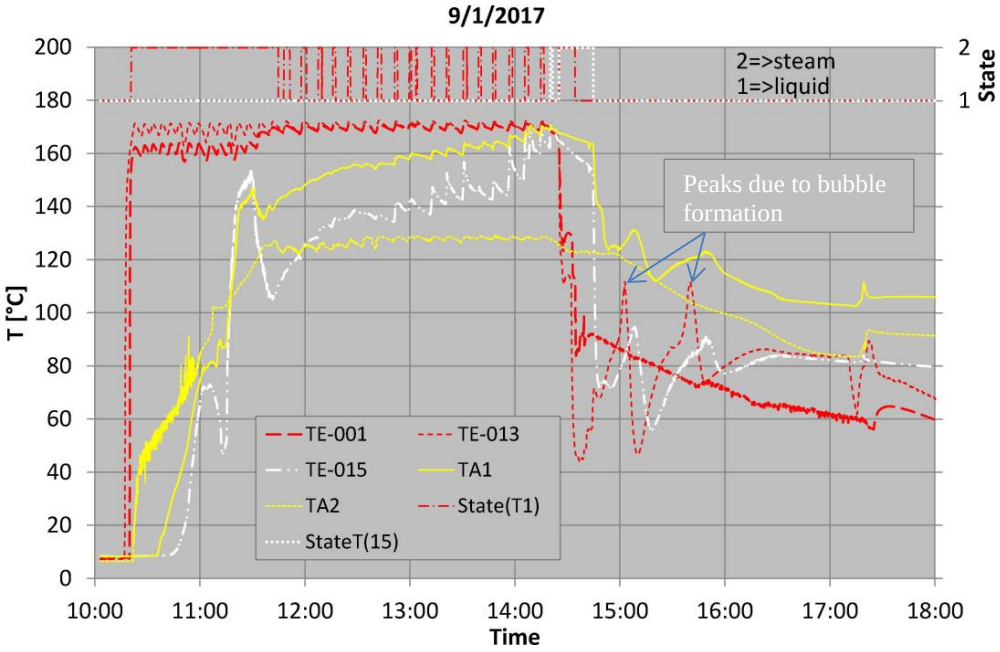

Fig. 3: Charging and discharging operation

In charging processes the steam generator continuously provides steam at 170 ºC and at a much lower pressure than 0.8 MPa, which is the saturation pressure at that temperature. Therefore, the mean HTF temperature within the module at its entrance increases with time as expected (TA1 and TA2 in Fig. 3). When the loop pressure was adjusted to get up to 0.8 MPa, the system reacts by changing the temperature at the outlet pipe of the module (TE-015) with a sudden drop down. Temperatures close to the outlet but within the module (TA1 and TA2) show a certain decrease, but not so important. When the gauge pressure becomes 0.4 MPa, the initial 0.025 kg/s steam decreases to 0.01 kg/s, which is in the range of the minimum steam mass flow the flowmeter can detect. 'State(T1)' variable shows if the water at the temperature (TE-001) prior to enter the storage module is steam (associated to value 2) or liquid (associated to a value 1). Working at pressures so close to saturation ones, implies that it may happen, as shown in Fig. 3, that steam is easily condensed prior to be supplied to the storage module.

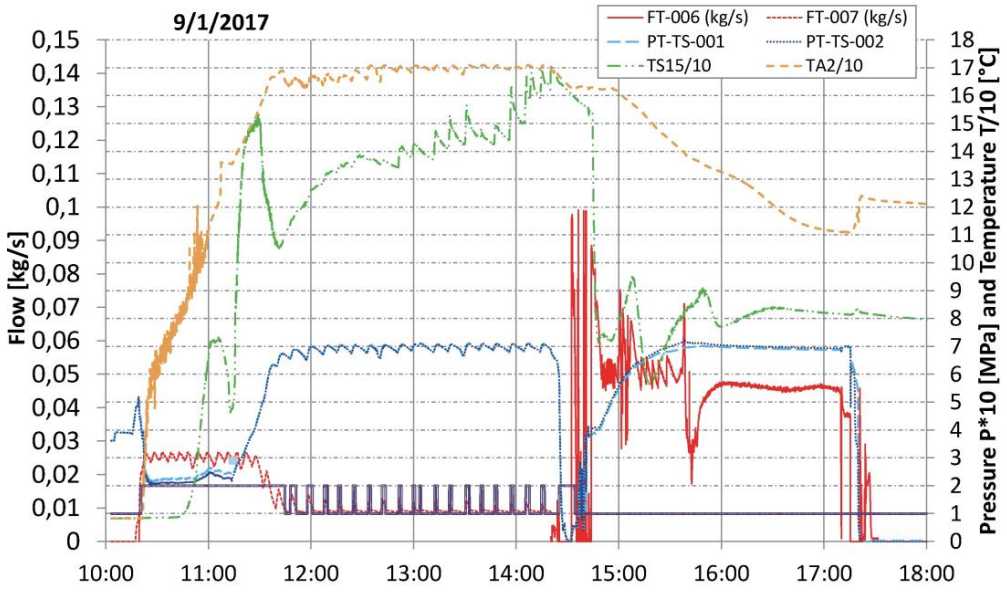

Fig. 4: Charging and discharging operation (flow, pressure and temperature/10)

3.2. Discharge mode

During the discharge, the operation takes place in the contrary flow direction: according to specifications saturated water at 130 °C enters the TES through the A1 conduction; being constant the power provided to the TES and producing, after evaporating in the TES, saturated steam at 130 °C. In this last case particular problems were found due to the electrical water heater used to preheat the water up to 130 °C, and finally, its set-point temperature had to be reduced to 85 °C in order to avoid an undesirable bubbles formation around the electrical resistance in the water heater. Temperature in the storage module was 160 °C, with a corresponding saturation pressure of 0.61 MPa, which is 0.2 MPa lower than the pressure in the circuit. Due to the imposed pressure loop, the water exiting the TES during the discharge is in liquid phase, even after exchanging enough energy with the PCM to be evaporated. Therefore, the foreseen methodology of testing and evaluation for discharging could not be applied.

3.3. Temperatures in the PCM

In the PCM channel of the storage module there are 6 thermocouples installed (see Fig.2): three in the central PCM channel (purple lines in Fig. 5) and another three close to the outer module surface at the opposite side at the horizontal entrance/exit of the HTF to the module (yellow lines in Fig. 5). These temperatures should reflect the fact that the PCM changes phase at a certain point.

According to the HITEC® study reported at 4.2 below, during charging (melting process) two phase transitions should be observed in the PCM: one at 90 ºC –which may correspond to a solid to solid transition- and another one at 140 ºC –corresponding to solid to liquid phase change-. The transition at around 90 ºC is observed in all these 6 thermocouples by a change in their profile slope. The 140 ºC transition is clearly observed only in TE-024. TE-027 may show a short of changing slope at that temperature but due to the fluctuations in the data it cannot be assured with certainty. TE-022 shows a transition but at around 130 ºC and TE-023, TE-025 and TE-026 seem to have no more transition but the one at 90 ºC.

During discharging (freezing the PCM) the above mentioned study supports to have two transitions: one at 140 ºC (liquid to solid) and another one at 60 ºC (corresponding to solid to solid phase change). The difference in the temperature at which the solid to solid transition takes placed is due to the supercooling effect. In discharging is the solid to liquid transition the one that is clearly identified in all the thermocouples that achieved 140 ºC. TE-024, TE-025 and TE-026 in the 9/1/2017 test, which is being used as example, do not reach but 160 ºC when the recording of experimental data stopped.

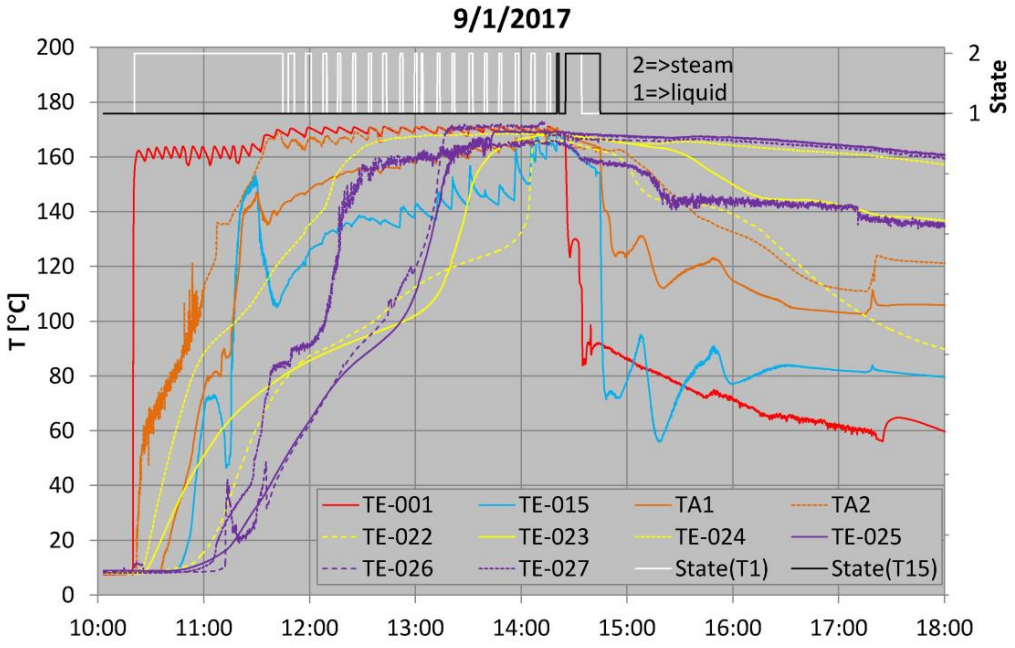

Fig. 5: PCM temperatures for charging and discharging on 9/1/2017.

During **charging**, temperature at the bottom (TE-022) and the top (TE-024) show the same profiles up to around 90 ºC, from which the steam boiler starts providing non-continuous steam at low mass flow and the value of the temperature gauges at the top began to increase more slowly than the bottom ones, reaching the solid to liquid transition temperature –around 140 ºC- 36 minutes later. This delay can be explained by considering that the steam supplied to the module stagnates at the upper part and, since steam has a poor heat transfer coefficient without changing phase, the PCM at this upper part requires more time to reach the same temperature level than at the bottom part when it condensate.

This inhomogeneous melting of the PCM within the storage module imposes a problem when determining the end of charging process. Depending on the period of time considered for charging, one of the following situations can occur at that point: part of the PCM at the top is still solid; part of the PCM at the bottom is superheated; or part of the PCM at the top is still solid and part at the bottom is superheated.

Looking at the temperatures or the state of the HTF at the exit of the storage module during charging (TE-016), this question is not clarified either. The end of charging may be assumed when steam is detected at the exit of the storage module; in this case the PCM gauges show a superheating behavior coming close and to around 170 ºC.

Discharging is assumed to start after a transition time, in which valves are closed/open to change to discharging HTF loop. In the case of the tests performed on 9/1/2017, at 15:37 pressure at the loop reaches 0.7 MPa but the cold mass water flow does not stabilized till 15:58 (see Fig. 4), thus discharging is assumed to start at that time. As mentioned in 3.1, due to the affordable loop pressure the water during discharge cannot be converted to steam, therefore the state of the corresponding HTF at the storage module exit does not give any clue on the end of discharging process.

Looking at PCM average temperatures, we can see that the three average profiles decrease their values with a different velocity as it happens during charging. While the PCM at the bottom of the storage module achieved the solidification temperature, 140 ºC, the PCM at the top of the module did not achieve such temperature when we stopped recording experimental data.

3.3. Thermal losses analysis

Idle thermal losses were expected to be calculated by the difference in discharged energy from a fully to a partially charged TES module situation, coming the partially charged situation from leaving the TES module for a certain time without any manipulation. As already mentioned, stablishing the end -and thus the associated energy- in a discharge process is not reliable due to the inhomogeneous behavior of the PCM. Thus, another procedure has to be applied.

One method for calculating idle thermal losses is to turn off all heating sources and track the rate of temperature

decay in average along certain time. By knowing the mass and enthalpy of storage media in the vessel, an estimation of the heat losses can be made by calculating the enthalpy variation in water and PCM from the starting time to the final time.

In Fig. 6 experimental results of the evolution of temperature during one week is shown. In those testing days some adjustments to the data acquisition system were performed so data is not continuously recorded along the whole day. These experimental data (- markers) is linked between them by an interpolation line. In this Figure, several "plateaus" at different temperatures can be observed for both water and PCM. It has been assumed that these plateaus are the result of a phase change occurring in the influence volume of the corresponding thermocouple. When the thermocouple is inserted in the PCM, the plateaus do not correspond necessary to its expected solid to liquid (around 140 °C) nor to its solid to solid (around 60 ºC) transitions, but keeps its temperature constant because some PCM around changes phases in spite that the PCM directly in contact does not. This assumption is a certainty with the thermocouples placed in water: no phase change takes place in the water at certain time period, but a plateau can be observed due to the phase change occurring in the adjacent PCM.

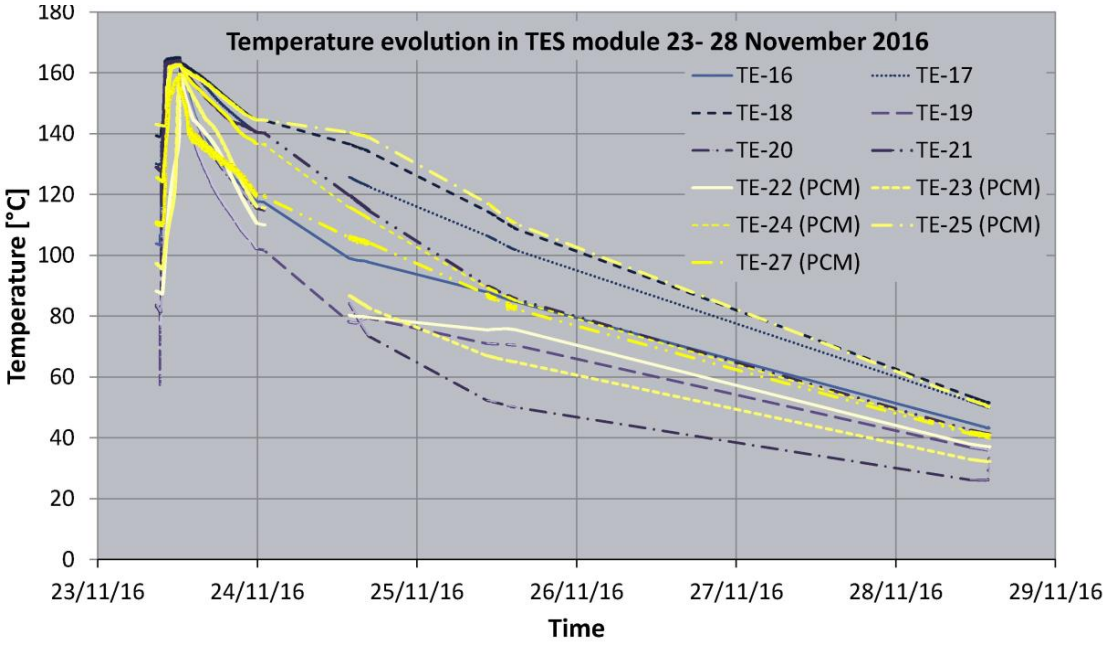

Fig. 6: Temperature evolution of water and PCM during the thermal losses test.

From these data, an estimation of 1.45 kW power thermal losses mean value has been found. This value is calculated by adding the thermal losses associated to the stainless steel conforming the TES module (25.6 kWh), the thermal losses of the PCM (23 kWh), those of the water (127.871.05 KWh) and knowing that these thermal losses have occurred along 121.78 hours. For sake of simplicity, ambient temperature has been considered the mean ambient temperature during the experiment (20 °C).

According to the authors, this method of calculating idle thermal losses by adding the idle thermal losses of the different components of the tank along a long period of time is the only possible way of calculating thermal losses of the while system, since it is not possible to define a representative temperature nor of the prototype nor of its surface in contact with ambient. This fact implies that it is not possible calculating a heat lost coefficient for a given TES module temperature (or time step) but just a mean value along a long period of time.

3.4. Charging and discharging power and stored energy

As already mentioned there is not a clear definition of the points at which charging and discharging processes end, since the storage module does not behave as a whole.

In Figure 7 the charging power for 9/1/2017 is shown. It is calculated by the mass flow measurement and the enthalpy change given by the HTF outlet conditions and HTF inlet conditions. Keeping in mind that the steam boiler provides steam at pulses, the obtained shawtooth profile is expected. The very low values from 11:25 onwards are due to the already mentioned decrease in steam mass flow production due to pressure loop and the limitations of the steam boiler. If there were not these disadvantages, a constant charging power would be expected.

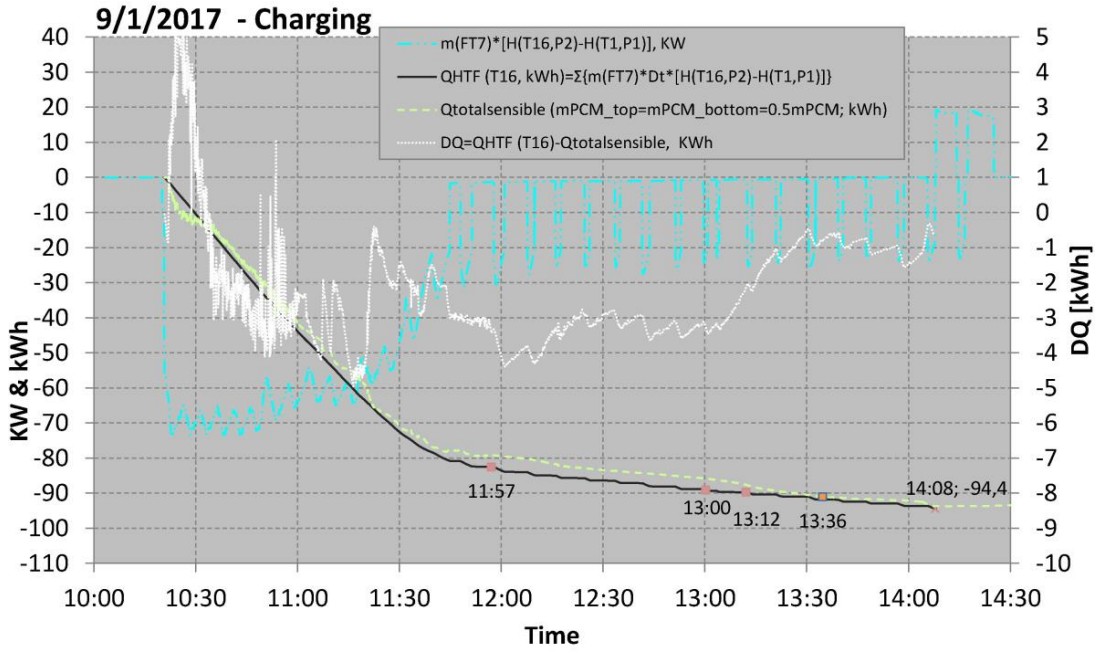

Fig. 7: HTF charging power, energy supplied by the HTF and estimated energy used for sensible heat.

In order to calculate the energy supplied by the HTF to the storage module, the above mentioned curve has been integrated in time (Q_{HTF}(T16), [kWh]). At the end of charging process, the HTF has supplied around 94.4 kWh to the whole system. Part of this energy has been used for increasing the temperature of the storage module ($Q_{sensible}$), [kWh], part for dealing with thermal losses (Q_{lost}),[kWh], and part has been stored in form of latent heat, by changing the phase of the PCM from solid to liquid (Q_{latent}), [kWh], i.e.,

$$Q_{HTF} = Q_{sensible} + Q_{lost} + Q_{latent} \qquad \text{(eq. 1)}$$

The sensible energy required to increase the temperature, $Q_{sensible}$, takes into account that the storage module is made of 1410 kg stainless steel (c_p=500 kJ/kgK) and 410 kg of HITEC (c_p=1560 kJ/kgK), which means that steel mass is more than 3 times PCM mass, while its heat capacity is around three times lower, giving similar thermal losses for both materials.

Considering that, as mentioned above, that mean heat loss power is 1.45 kW, the resulting energy for the latent heat is 1 kWh, which implies 9 kJ/kg specific latent heat of the PCM, which is much lower than the one expected up to now. This result makes Hitec salt not the most appropriate candidate for its use as PCM.

The main conclusion obtained is that with a module of this type it is necessary to know with certain accuracy a thermal map of the PCM. The storage module tested here did not allow including temperature gauges at different radial positions, but at the center and outer radius of the equipment. This would allow a better definition of the phase change moment for the different parts of the TES module, since one of the main conclusions of this work is the difficulty in defining ends of charging and discharging processes when inhomogeneous phase change processes take place.

4. Performance studies of Hitec® salt

As stated in a previous work (Rodríguez-García and Rojas, 2016), the selected PCM implemented in the spiral storage module was the commercial eutectic salt mixture Hitec® ($NaNO_3$-KNO_3-$NaNO_2$; 7/53/40 % w) (http://www.coastalchem.com/). This salt mixture has the melting point at 142 °C with a reported enthalpy of fusion of about 83 kJ/kg and is expected to be thermally stable up to 535 °C (http://stoppingclimatechange.com). Despite its relatively low phase change enthalpy, this salt was finally selected because its melting temperature fits the operating temperature range of the storage module but also because it has proven to be chemically stable upon daily melting/freezing cycles under inert atmosphere (Rodríguez-García and Rojas, 2016).

4.1. DSC measurements

For a preliminary stability study a Hitec® sample previously dried at 120 ºC for 48 hours was subsequently cycled between 130 ºC and 150 ºC at 2 ºC/min except for the first heating that was performed at 10 ºC/min. The resulting

curves are plotted in Fig.8 and the temperatures and enthalpies calculated for each cycle are recorded in Tab. 2.

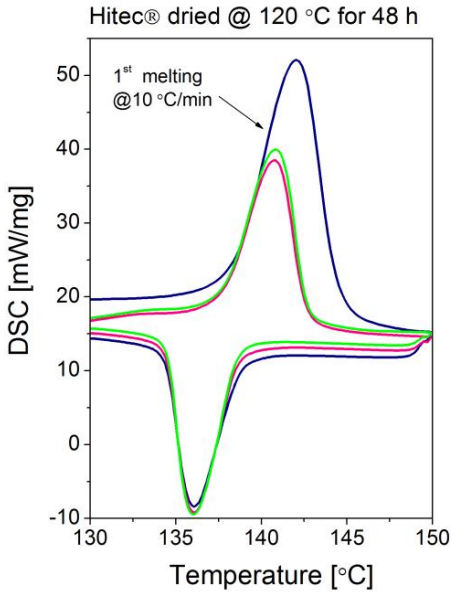

Fig. 8: Three DSC melting/freezing cycles performed from 130 °C to 150 °C for Hitec® commercial mixture dried at 120 °C for 48 h.

Tab. 2: Results of DSC measurements displayed in Fig. 8

Cycle	$T_{melt-peak}$	ΔH_{melt}	$T_{freez-peak}$	ΔH_{feez}
1st	142 ºC*	56 kJ/kg*	136 ºC	51 kJ/kg
2nd	141 ºC	57 kJ/kg	136 ºC	49 kJ/kg
3rd	141 ºC	60 kJ/kg	136 ºC	47 kJ/kg
(*) Performed at 10 ºC/min				

As we can see thermal behavior is maintained during cycling and not only in terms of temperatures but also in terms of enthalpies. In this way, the mean melting temperature obtained is about 142 ºC while the freezing temperature is 136 ºC. This small difference between melting and freezing is usually observed in DSC measurements and does not correspond to any supercooling phenomenon. As for the enthalpy values they remain constant for all cycles being the values slightly higher for melting (57 kJ/kg) than for freezing (49 kJ/kg). It is important to remark that the melting enthalpy obtained experimentally is no higher than 60 kJ/kg and hence rather lower than the expected theoretical value of 80 kJ/kg. On the other hand the peak of the first heating cycle is much larger than the other peaks because this run was performed at 10 ºC/min and the others at 2 ºC/min. However the thermal result of this run is similar to the results of the other ones.

DSC measurements were also performed for Hitec® salt previously dried at 120 ºC for 48 hours in the temperature interval 50 ºC-160 ºC at 10 ºC/min rate. The curves obtained for the first heating and the second heating /cooling runs are displayed in Fig. 9. During the first heating run, we observe a sharp peak at around 131 °C that could correspond to adsorbed water evolution together with a broad peak corresponding to the melting of the bulk salt powder. During the first DSC run not much information about sample thermal properties can be obtained since the main goal is to make it homogeneous. During the second heating/cooling runs, if temperature is decreased down to 50 ºC, in addition to the melting/freezing process at ~140 ºC other transition is observed at 93 ºC upon heating and at 119 ºC upon cooling. It is interesting to note that the additional transition observed in the heating run (at 93 ºC) has an enthalpy almost in the range of the melting process. This would explain the plateau displayed by some of the thermocouples recording temperatures inside the REELCOOP P#3 storage prototype at a temperature lower than the melting one.

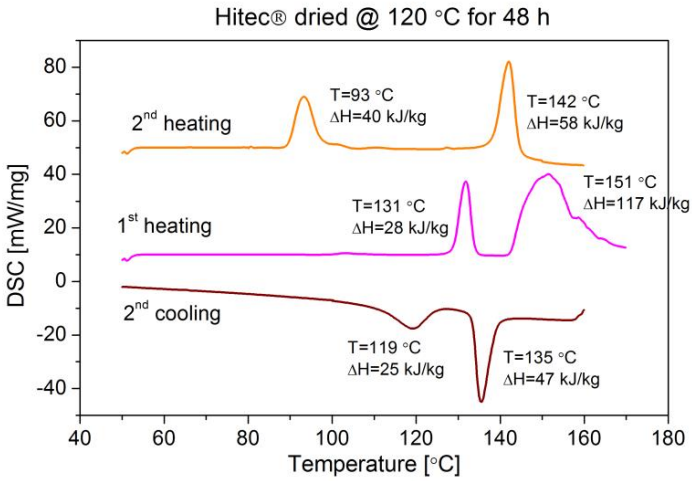

Fig. 9: DSC curves for 1st heating and 2nd heating/cooling runs for HITEC® mixture previously dried @ 120 ºC for 48 h.

4.2. Thermal cycles under air

In order to confirm that Hitec® has a transition that takes place at a temperature lower than the melting one, various daily heating/cooling cycles between 40 ºC and 170 ºC were performed under air in an oven with forced ventilation and hence with strict temperature control. Fig. 10 displays one of these cycles where it can be seen not only a shoulder at around 140 ºC that corresponds to the eutectic phase change but also other shoulder at lower temperature with apparently similar size. The shoulder associated to the melting/freezing transition appears at the same temperature during both heating and cooling processes, which confirms that Hitec® does not present supercooling. For the shoulder at lower temperature we can see that it appears at 90 ºC during the heating and at 60 ºC during the cooling. This is in agreement not only with the plateaus observed at around 90 ºC in the temperature curves recorded during the charging of REELCOOP P#3 storage prototype (Fig. 1.b) but also the DSC heating scan of Fig. 9. The fact that this transition appears at a lower temperature (60 ºC) during the cooling can be due to a supercooling phenomenon. This can be the reason why it was not observed in DSC scans since they were only performed down to 50 ºC and usually supercooling effect is larger in this kind of measurements due to the small amount of sample they use. On the other hand, since the oven has forced ventilation and Hitec® remained melted at 170 ºC for about 10 h and hence enough time and temperature to evolve any adsorbed water, this low temperature shoulder can be more likely associated to a solid to solid transition than to water exchange.

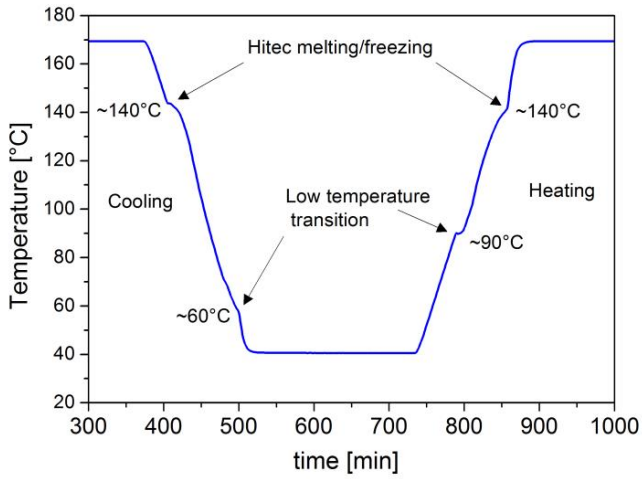

Fig. 10: Close view of a temperature-time curve for a daily heating/cooling cycle of a Hitec® sample between 40 ºC and 170 ºC.

4.3. Studies of thermal degradation

Hitec® salt is not a medium chemically stable since its components can react between them or with their environment (atmosphere or metallic walls) through processes strongly temperature dependent. One of the widest studies of Hitec® thermal degradation was published by Roche in 1980. This author observed that the main indicator of Hitec® degradation is the decrease of nitrite ions which leads to an increase of melting temperature in the salt mixture. Actually if all nitrites were converted in nitrates the final salt composition would be the eutectic mixture $NaNO_3$-KNO_3 47/53 %-w whose melting point is 220 ºC.

According to Roche 1980, the main degradation reactions of Hitec® mixture are the following:

$$(Na,K)NO_2 + \frac{1}{2}O_2 \leftrightarrow (Na,K)NO_3 \qquad \text{(eq. 2)}$$

$$5(Na,K)NO_2 \leftrightarrow 3(Na,K)NO_3 + (Na,K)_2O + N_2 \qquad \text{(eq. 3)}$$

The first one (eq. 2) is the oxidation of nitrite to nitrate by the oxygen, which is expected to take place in open systems exposed to air, whereas the second one (eq. 3) is the so called nitrite *thermolysis* in which nitrate, oxide and nitrogen are produced. In this case the presence of oxygen is not required and hence this reaction can take place in closed systems.

Assuming that only these two reactions are involved in Hitec® degradation, Roche (1980) obtained the thermodynamic equations governing the equilibrium and with them he calculate the mole percentage of all species involved in the equilibrium (nitrites, nitrates and oxides) as function of temperature for different environments. In this way, when molten Hitec® is kept under air at temperatures below 500 ºC, the predominant species are the nitrates and hence the risk of nitrite oxidation is very high. However, at temperatures above 500 ºC, nitrites become more stable and reaction (2) can even be reversed with the corresponding evolution of oxygen. For the case of oxides they start only appearing above 850 ºC. In contrast, if molten Hitec® is kept under N_2 with a very little amount of oxygen (0.001 atm) the amount of nitrites at 500 ºC increases dramatically (from 2.6 % in air to 27.3 % in N_2), which are good news, whereas oxides can appear already at 600 ºC increasing the corrosion risk and the possibility of other degradation reactions (Roche, 1980). It must be taken into account that these results correspond to the equilibrium composition of the molten Hitec but thermodynamic equations do not give any information about how long it takes until such equilibrium state is reached. For that information the kinetics of these degradation reactions must be studied.

In this way Olivares (2012) performed kinetic studies of Hitec® thermal degradation under different gas atmospheres by means of thermogravimetric analysis. In general it can be said that Hitec® seems to be stable under any gas atmosphere for temperatures lower than 370 ºC and this stability range is extended to about 470 ºC if it is kept under inert atmosphere (Ar or N_2). Under either O_2 or air atmospheres nitrites undergo slow oxidation at 370 ºC-390 ºC through eq. 2 but this process is not observed when inert gases are used. However, for all atmospheres once 450-500 ºC is reached, gas emission is produced although the strong weigh loss begins at about 610 ºC. The gases evolved during weight loss are NO, NO_2, O_2,, N_2, which are the expected products of both nitrate and nitrite thermal degradation. Roche 1980 also performed various test for determining Hitec® degradation rate under different atmospheres by monitoring the variation of NO^{2-} molar percentage versus the number of days it had been kept at a certain temperature. Again they obtained that degradation of Hitec® starts to be important at temperatures above 300 ºC not only under N_2 but also under air atmosphere. However, due to the operating conditions of the storage module of REELCOOP P#3 prototype, the highest working temperature of molten Hitec® is not expected to exceed 180 ºC. Therefore kinetic results of Olivares 2012 and Roche 1980 are not valid in our case. Moreover, the degradation experiments performed by both authors were not correlated to any kinetic equation and hence their extrapolation to low temperature region cannot be done directly.

Fortunately, it has been found in the literature that Freeman described the degradation kinetics of both $NaNO_2$/$NaNO_3$ (Freeman 1956) and KNO_2/KNO_3 systems (Freeman 1957) with similar equations. Therefore we can assume that the same expressions could be used for describing the thermal degradation of Hitec® mixture. By combining the experimental results of Roche (1980) and the kinetic equations of Freeman (1956 and 1957) for nitrites degradation, it was possible to obtain the dependence of the kinetic constant with temperature and hence estimate the degradation of Hitec® under air at temperatures close to the melting point. As displayed Fig. 11.a, in the time scale of a year, Hitec® mixture undergoes strong degradation under air when kept at temperatures higher than 400 ºC whereas for operation temperatures of 300 ºC, nitrite mole fraction remains at its initial value (0.49). When degradation curves of Hitec® are calculated for lower temperatures (see Fig. 11.b), degradation time scale has to be increased to several years. In this case we can see that for temperatures below 200 ºC, Hitec® shows no

decrease in nitrite content and hence no significant degradation should be expected for at least 10 years of operation in that temperature range.

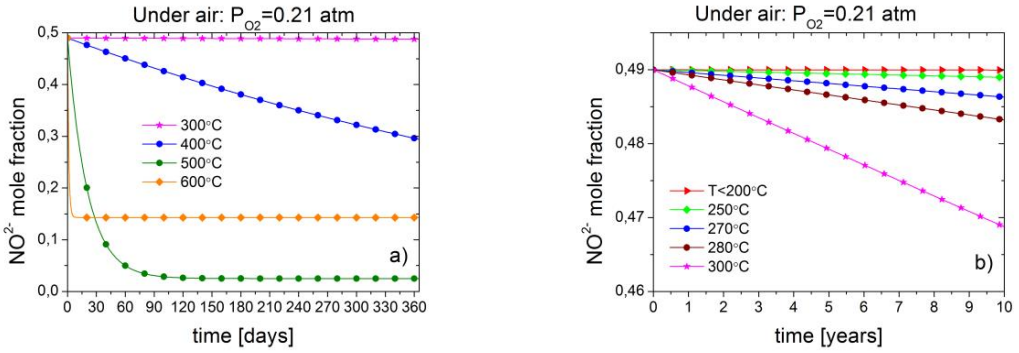

Fig. 11: Expected Hitec® degradation under air in the temperature range: 600 ºC-300 ºC (a) and in the range: 300 ºC-200 ºC (b).

From these calculations we can conclude that Hitec® mixture can be kept under ambient air without any risk of degradation due to nitrite oxidation when used as PCM for latent storage in the range of its melting temperature. However, although salt degradation is not expected in the presence or air, the metallic container might not behave in the same way and hence undergo corrosion due to the presence of air or to the molten salt itself. This could change the behavior of Hitec® salt and promote its degradation. This was one of the reasons why REELCOOP P#3 prototype inner cavity was kept under N_2 in order to avoid any atmosphere undesirable degradation process either in the salt or in the material container. The other reason was preventing moisture to be in contact with Hitec® mixture since we observed that it is quite hygroscopic in solid state.

In order to confirm that no degradation happened in Hitec® salt upon short-term cycling, we analyzed the composition of some samples by ionic chromatography before and after either consecutive or daily cycles performed under air or inert atmosphere (N_2 or Ar). The results in terms of ionic weight percentage are recorded in Tab. 3. The analysis of ionic composition of Hitec® showed a slight decrease of nitrite concentration after 50-60 daily melting/freezing cycles. However, the increase in nitrate composition is not so clear especially if we take into account that cation percentages do not remain constant. Hence, since the values are close to the theoretical ones, these variations could be within the limits of the experimental error specially if we take into account that the results for the cycles under air are the same as the results for the cycles under inert atmosphere.

Tab. 3: Results of Hitec® analysis by means of ionic chromatography.

	Na^+[w-%]	K^+[w-%]	NO_3^-[w-%]	NO_2^-[w-%]
Theoretical composition	15.2	20.4	37.6	26.7
As received Hitec® salt	17	18	33	31.7
After 5 consecutive cycles in air	16	20	36.5	28.7
After 25 consecutive cycles in air	16	19	35.8	28
After 60 daily cycles in air	17	20	37.4	26.7
After 50 daily cycles in N_2	17	20	37.5	25.8
After 53 daily cycles in Ar	17	20	37.3	26

5. Conclusions

In this article the experimental results of the REELCOOP project have been evaluated. In this project a PCM thermal energy storage with a spiral geometry is used. In terms of the behaviour of the storage prototype, it can be said that inhomogeneous melting/solidification processes of the PCM takes place due to the stagnation of steam in the upper part of the module. This inhomogeneous melting/solidification processes implies that the charging and discharging processes are difficult to be defined and limited in time, which results in not very accurate charge and discharge power and thermal losses calculations.

The obtained values for power and stored energy are much lower than the expected ones: 50 kWth as the lowest expected power against the 13 kWth as the largest experimentally calculated; 6 kWh expected thermal capacity against 1 kWh experimentally observed. This mismatch may be due to a lower specific latent heat of the PCM (9 kJ/kg) than the expected from DSC measurements (around 50 kJ/kg).

In spite of a well-designed insulation not only around the prototype but also by reducing thermal bridges by having two well-isolated storage module supports, thermal losses are 1.44 kW. Thermal losses related to the steel (tank and channeling) are of the same order as the ones of the PCM.

Considering the above, we have to conclude that neither the module design nor the PCM are appropriate options for storing latent energy.

The performance studies carried out Hitec® have shown that this salt does not display supercooling while its corresponding melting enthalpy is much lower than the reported value (55 kJ/kg vs. 80 kJ/kg). Hitec also displays an additional transition at a temperature lower than the melting temperature which is most probably associated to a solid-solid and not to water evolution. Kinetic calculations and salt analysis after short-term cycling have demonstrated that Hitec® was not expected to degrade due to nitrite to nitrate conversion during the prototype testing period.

The mismatch between the results obtained of the PCM at laboratory level -with small amounts of PCM and well controlled ambient conditions- and those obtained in a medium size storage module shows the importance of manufacturing prototypes and avoid claiming feasibility of materials for storing energy just by laboratory results.

6. Acknowledgements

The authors would like to acknowledge the E. U. through the 7th Framework Program for the financial support of this work under the REELCOOP (Renewable Electricity cooperation) project with contract number: 608466, the DETECSOL project (Ref. ENE2014-56079-R) with ERDF funds, and the operation, instrumentation and maintenance departments at the PSA for their collaboration during the development of this work

7. References

Freeman E. S., 1956. The kinetics of the thermal decomposition of sodium nitrate and of the reaction between sodium nitrite and oxygen, Journal of Physical Chemistry 60 (11), 1487-1493.

Freeman E. S., 1957. The kinetics of the thermal decomposition of potassium nitrate and of the reaction between potassium nitrite and oxygen, Journal of the American Chemical Society 79 (4), 838-842.

Olivares R., 2012. The thermal stability of molten nitrate/nitrite salt for solar thermal energy storage in different atmospheres. Solar Energy 86, 2576-2583.

Rivas E., Rojas E., Bayón R., inventor, Ciemat, assignee. 2011 Aug. 11. Módulo de almacenamiento térmico basado en calor latente con altas tasas de transferencia de calor. Spanish patent P201131378.

Roche M., 1980. L'utilisation d'un mélange de sels fondus pour le stockage de chaleur, Revue Phys. Appl. 15, 895-902.

Rodríguez-García M.M., Bayón R., Rojas E., 2016a. Stability of D-mannitol upon melting/freezing cycles under controlled inert atmosphere. Energy Procedia 91, 218-225.03

Rodríguez-García M.M., Rojas, E. 2016b. Testing a new design of latent storage. 11th ISES EuroSun 2016, International Conference on Solar Energy for Buildings and Industry. Palma de Mallorca, Spain. 11-14 October 2016.

Rojas et al., 2011, Definition of standardised procedures for testing thermal storage prototypes for concentrating solar thermal plants. SFERA project. Available at http://sfera.sollab.eu/downloads/JRA/WP15/Deliverable15.2_StandardisedTestingProcedures.pdf

http://stoppingclimatechange.com/MSR%20-%20HITEC%20Heat%20Transfer%20Salt.pdf